Title

Genetic deletion of the mitochondrial phosphate carrier desensitizes the mitochondrial permeability transition pore and causes cardiomyopathy.

Journal

Cell death and differentiation, 21(8)

ISSN

1350-9047

Authors

Kwong, JQ
Davis, J
Baines, CP
et al.

Publication Date

2014-08-01

DOI

10.1038/cdd.2014.36

Cell Death and Differentiation (2014) 21, 1209–1217

www.nature.com/cdd

Genetic deletion of the mitochondrial phosphate carrier desensitizes the mitochondrial permeability transition pore and causes cardiomyopathy

JQ Kwong[1], J Davis[1], CP Baines[2], MA Sargent[1], J Karch[1], X Wang[1], T Huang[1] and JD Molkentin*[,1,3]

The mitochondrial phosphate carrier (PiC) is critical for ATP synthesis by serving as the primary means for mitochondrial phosphate import across the inner membrane. In addition to its role in energy production, PiC is hypothesized to have a role in cell death as either a component or a regulator of the mitochondrial permeability transition pore (MPTP) complex. Here, we have generated a mouse model with inducible and cardiac-specific deletion of the *Slc25a3* gene (PiC protein). Loss of PiC protein did not prevent MPTP opening, suggesting it is not a direct pore-forming component of this complex. However, *Slc25a3* deletion in the heart blunted MPTP opening in response to Ca^{2+} challenge and led to a greater Ca^{2+} uptake capacity. This desensitization of MPTP opening due to loss or reduction in PiC protein attenuated cardiac ischemic-reperfusion injury, as well as partially protected cells in culture from Ca^{2+} overload induced death. Intriguingly, deletion of the *Slc25a3* gene from the heart long-term resulted in profound hypertrophy with ventricular dilation and depressed cardiac function, all features that reflect the cardiomyopathy observed in humans with mutations in *SLC25A3*. Together, these results demonstrate that although the PiC is not a direct component of the MPTP, it can regulate its activity, suggesting a novel therapeutic target for reducing necrotic cell death. In addition, mice lacking *Slc25a3* in the heart serve as a novel model of metabolic, mitochondrial-driven cardiomyopathy.
Cell Death and Differentiation (2014) **21,** 1209–1217; doi:10.1038/cdd.2014.36; published online 21 March 2014

The mitochondrial oxidative phosphorylation (OXPHOS) system is the primary source of cellular energy production. Defects in OXPHOS occur with a frequency of 1 in 5000 live births[1] and underlie a wide range of mitochondrial disorders that often affect multiple organ systems and tissues with high oxidative energy demands, such as brain, skeletal muscle, and heart.[2] Cardiac phenotypes associated with mitochondrial disease are diverse, and can range from cardiomyopathies to cardiac conduction defects.[3–5]

The mitochondrial phosphate carrier (PiC) is a member of the solute carrier 25A family that has a critical role in OXPHOS, serving as the primary route for inorganic phosphate (Pi) import into the mitochondrial matrix.[6,7] PiC, together with the adenine nucleotide translocator (ANT) and the ATP synthase, forms the ATP synthasome whereby all of the metabolites needed to generate ATP are within one immediate microdomain.[8,9] The importance of PiC in facilitating energy production is highlighted by the profound disease phenotype observed in patients presenting with mutations in the skeletal muscle-specific isoform of this gene.[10,11] Such patients present with a multisystemic disorder characterized by muscle hypotonia, lactic acidosis, severe hypertrophic cardiomyopathy, and shortened lifespan.[10,11] Similarly, patients with *SLC25A4* (ANT1 protein) deficiency present with cardiomyopathy,[12] as do mice lacking the *Slc25a4* gene,[13] likely due to a similar molecular defect in the efficiency of ATP production within the mitochondria.

In addition to its role in mitochondrial energy metabolism, PiC has been implicated in regulating cell death by serving either as a modulator or a direct component of the mitochondrial permeability transition pore (MPTP).[14–16] The MPTP is a non-selective channel that forms in response to Ca^{2+} overload and oxidant stress that allows inner-membrane permeability to solutes up to 1500 Da in size, leading to loss of mitochondrial membrane potential, mitochondrial swelling and rupture, and eventually cell death through necrosis.[15] Structurally, the MPTP complex has been proposed to be comprised of the ATP synthase[17,18] and to be regulated by cyclophilin D (CypD),[19,20] ANT,[21] and the pro-apoptotic proteins Bax and Bak in the outer mitochondrial membrane.[22,23] PiC has also been suggested to be an inner-membrane component of the MPTP because it can form nonspecific channels in lipid membranes and because the MPTP is known to be activated by Pi.[24–27] Finally, PiC directly interacts with CypD in the mitochondrial matrix, which is a verified regulator and component of the MPTP.[16] *Saccharomyces cerevisiae* lacking PiC have altered MPTP characteristics with a smaller pore size, suggesting it might

[1]Department of Pediatrics, Cincinnati Children's Hospital Medical Center, University of Cincinnati, Cincinnati, OH, USA; [2]Dalton Cardiovascular Research Center, University of Missouri-Columbia, Columbia, MO, USA and [3]Howard Hughes Medical Institute, Cincinnati Children's Hospital Medical Center, Cincinnati, OH, USA
*Corresponding author: JD Molkentin, Molecular Cardiovascular Biology Division, Howard Hughes Medical Institute, Cincinnati Children's Hospital Medical Center, 240 Albert Sabin Way, MLC 7020, Cincinnati, OH 45229, USA. Tel: +1 513 636 3557; Fax: +1 513 636 5958; E-mail: jeff.molkentin@cchmc.org
Abbreviations: α-MHC, α-myosin heavy chain; AdCre, adenovirus-expressing Cre recombinase; Adβgal, adenovirus-expressing β-galactosidase; ANT, adenine nucleotide translocator; ATR, atractyloside; CypD, cyclophilin D; CsA, cyclosporine A; fl, loxP site; MCM, αMHC-MerCreMer transgene; MEFs, mouse embryonic fibroblasts; MPTP, mitochondrial permeability transition pore; Pi, inorganic phosphate; PiC, mitochondrial phosphate carrier; OXPHOS, mitochondrial oxidative phosphorylation; ROS, reactive oxygen species; SR, sarcoplasmic reticulum; WT, wild type
Received 24.10.13; revised 14.2.14; accepted 17.2.14; Edited by N Chandel; published online 21.3.14

directly participate in the mitochondrial permeability pore.[28] However, partial reduction of PiC by siRNAs in cultured cells had no effect on mitochondrial permeability activity, suggesting that PiC is not required for MPTP function.[27] Definitive genetic proof of PiC's involvement in MPTP formation/function is currently lacking.

In the present study, we tested the role of PiC in MPTP regulation and cell death *in vivo* using a mouse model with inducible cardiomyocyte-specific deletion of the *Slc25a3* gene (encodes PiC). We found that cardiac mitochondria depleted of PiC were able to undergo permeability transition, suggesting that PiC is not a requisite component of the MPTP. However, the extent of Ca^{2+}-induced MPTP opening was blunted, suggesting that PiC serves to regulate this activity. Furthermore, *Slc25a3* deletion produced a unique mouse model of mitochondrial-driven hypertrophic cardiomyopathy that recapitulates features observed in human patients with phosphate carrier deficiency and metabolic cardiomyopathy.

Results

Generation of mice with an inducible cardiac myocyte-specific deletion of *Slc25a3*. To determine the necessary role of PiC in the heart, gene-targeted mice were generated from embryonic stem cells in which the *Slc25a3* genetic locus was targeted with a DNA vector that after homologous recombination resulted in the placement of loxP sites (fl) flanking exons 1 and 2, to permit future conditional disruption of this gene in the mouse heart (Figure 1a). Inducible cardiac-specific deletion of *Slc25a3* was achieved by crossing *Slc25a3*$^{fl/fl}$ mice with transgenic mice expressing a tamoxifen-induced Cre protein, referred to as MerCreMer (MCM), under the regulation of the α-myosin heavy-chain (α-MHC) promoter (*Slc25a3*$^{fl/fl\text{-}MCM}$). Before tamoxifen induction, baseline cardiac dimensions and function were unchanged in *Slc25a3*$^{fl/fl\text{-}MCM}$ mice as compared with wild type controls, and the placement of the loxP alleles in the *Slc25a3* locus had no effect on PiC protein expression levels (Figure 1b). *Slc25a3* deletion was induced in adult 2-month-old mice by administering tamoxifen (25 mg/kg/day) for 5 days. PiC protein expression, as assessed by western blot analysis, was reduced by $>90\%$ in heart mitochondria from *Slc25a3*$^{fl/fl\text{-}MCM}$ mice as compared with controls, whereas other mitochondrial respiratory chain proteins and MPTP-related proteins such as CypD and the voltage-dependent anion channel were unaffected (Figure 1b).

Deletion of *Slc25a3* causes impaired mitochondrial ATP synthesis. To examine the acute metabolic effects of *Slc25a3* depletion, we isolated cardiac mitochondria 2 weeks after tamoxifen administration. Ablation of *Slc25a3* over this 2-week time period resulted in a significant decrease in the rate of mitochondrial Pi uptake (Figure 1c) that was accompanied by a $\sim$45% decrease in the rate of mitochondrial ATP synthesis compared with mitochondria isolated from various control hearts (Figure 1d). Notably, despite the impairment in mitochondrial ATP production, total cardiac tissue ATP levels were maintained (Figure 1e, see below). To confirm that the mitochondrial ATP synthesis defect was a primary effect of *Slc25a3* deletion as opposed to a consequence of respiratory chain dysfunction, we measured the activities of the individual respiratory complexes, which were unchanged in mitochondria isolated from hearts of *Slc25a3*$^{fl/fl\text{-}MCM}$ mice after 2 weeks of tamoxifen administration (Figure 1f). Mitochondrial reactive oxygen species (ROS) production was similarly unaffected, suggesting that uncoupling was not occurring in the absence of PiC protein (Figure 1g). Together, these results indicate that acute *Slc25a3* deletion causes impaired mitochondrial Pi uptake that leads to reduced mitochondrial ATP synthesis.

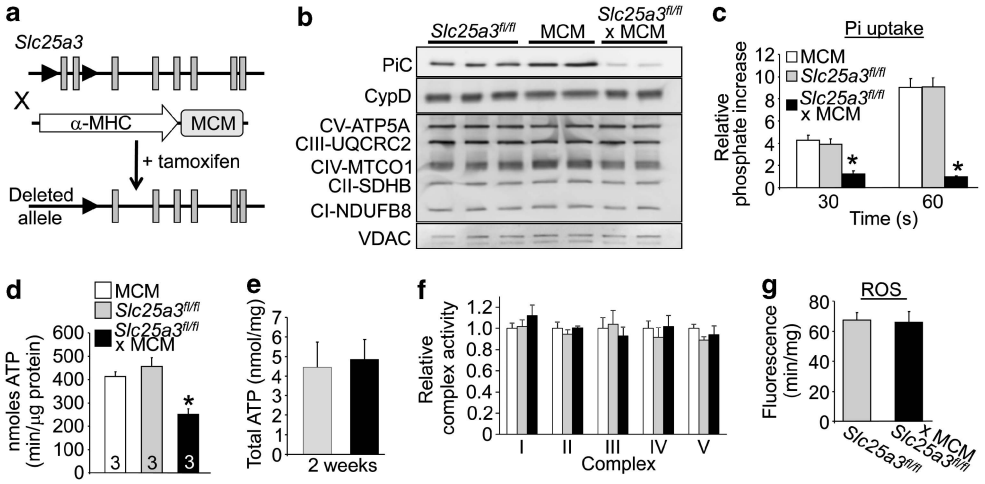

Figure 1 The effect of *Slc25a3* deletion over 2 weeks on cardiac mitochondrial bioenergetics. (**a**) Targeting strategy and resulting mice for the *Slc25a3* locus where exons 1 and 2 were flanked with loxP sites (triangles), which were then crossed with αMHC-MerCerMer (MCM) transgenic mice. Tamoxifen was given to activate the MCM protein and cause deletion of these exons. (**b**) Western blot of PiC, CypD, and OXPHOS complex subunits in cardiac mitochondria from hearts of the indicated mice. VDAC was used as a mitochondrial protein loading control. (**c**) Quantification of cardiac mitochondrial ^{32}P uptake (Pi). *$P<0.05$ *versus* all other groups. (**d**) Rate of mitochondrial ATP synthesis in isolated cardiac mitochondria from the indicated groups. *$P<0.05$ *versus* all other groups. (**e**) Quantification of ATP content in cardiac tissue from mice of the indicated genotypes ($n=3$ per group). (**f**) Enzymatic activities of the individual respiratory chain complexes from cardiac mitochondria of the indicated genotypes. (**g**) Mitochondrial H_2O_2 production as measured by Amplex Red, from hearts of the indicated genotypes. All values reported as mean $\pm$ S.E.M. fl/fl, homozygous *Slc25a3-loxP*-targeted mice

Short-term deletion of *Slc25a3* does not negatively impact cardiac structure–function. Despite the decrease in mitochondrial ATP synthesis observed in the *Slc25a3*$^{fl/fl\text{-}MCM}$ mice 2 weeks after tamoxifen-mediated deletion, echocardiographic and morphometric measurements showed only a very mild hypertrophic effect with no change in cardiac ventricular performance compared with controls (Figures 2a and b). In addition, cardiac myocyte and mitochondrial architecture assessed by electron microscopy were unaffected in hearts from *Slc25a3*$^{fl/fl\text{-}MCM}$ mice as compared with controls (Supplementary Figure S1). To examine the functional effects of abrogated PiC protein, we analyzed contractility of isolated cardiomyocytes from *Slc25a3*$^{fl/fl\text{-}MCM}$ and control mice 6 weeks after tamoxifen administration. Myocyte shortening and relaxation times were unchanged by loss of PiC protein as compared with controls (Figures 2c–e), consistent with the basic preservation in cardiac structure and function observed in *Slc25a3*$^{fl/fl\text{-}MCM}$ mice over this time period. To further examine the effects of PiC deletion on cardiac function, we measured calcium handling through the sarcoplasmic reticulum (SR) and the Ca^{2+} transient in cardiomyocytes isolated from *Slc25a3*$^{fl/fl\text{-}MCM}$ and control mice at 10 weeks following tamoxifen administration. Although PiC deletion resulted in increased SR Ca^{2+} load (Figure 2f), overall Ca^{2+} reuptake time was unchanged (Figure 2g). These results indicate that Ca^{2+} cycling in the PiC-deficient myocytes is maintained and even somewhat optimized as a potential contractile compensatory adaptation to offset lower ATP generation capacity from the mitochondria.

***Slc25a3* affects Ca^{2+} overload-induced MPTP opening and cell death.** Mitochondrial Pi is a known regulator of the MPTP[26] and PiC itself has been suggested to serve as an obligate structural component of the MPTP. Here we used the *Slc25a3*$^{fl/fl\text{-}MCM}$ model to genetically examine MPTP function in cardiac mitochondria lacking greater than 90% of PiC protein. Given that the acute 2-week depletion protocol described above did not adversely affect cardiac function, this time point was used to more carefully examine mitochondrial permeability transition and Ca^{2+} uptake. First, cardiac mitochondria isolated from *Slc25a3*$^{fl/fl\text{-}MCM}$ mice and controls were assessed for their ability to undergo MPTP-dependent swelling in response to Ca^{2+} overload and atractyloside (ATR), two known inducers of MPTP opening. Although both Ca^{2+} (200 μM) and ATR were able to induce swelling in mitochondria from hearts of *Slc25a3*$^{fl/fl\text{-}MCM}$ mice, the extent of Ca^{2+}-induced swelling was reduced by approximately half in PiC-depleted mitochondria compared with controls (Figures 3a and c). However, no reduction of swelling was observed with ATR because this agent induces MPTP formation through an effect on ANT activity, and more importantly, switching to a phosphate-free buffer with arsenate as the anion carrier eliminated this mild reduction in mitochondrial swelling from hearts of *Slc25a3*$^{fl/fl\text{-}MCM}$ mice when challenged with 400 μM Ca^{2+} (Figure 3b). These results suggest that PiC is not a direct pore-forming component of the MPTP complex. Importantly, cyclosporine (CsA), a known desensitizer of the MPTP, still inhibited Ca^{2+}-dependent swelling of heart mitochondria from all genotypes of mice (Figure 3a). Collectively, these results

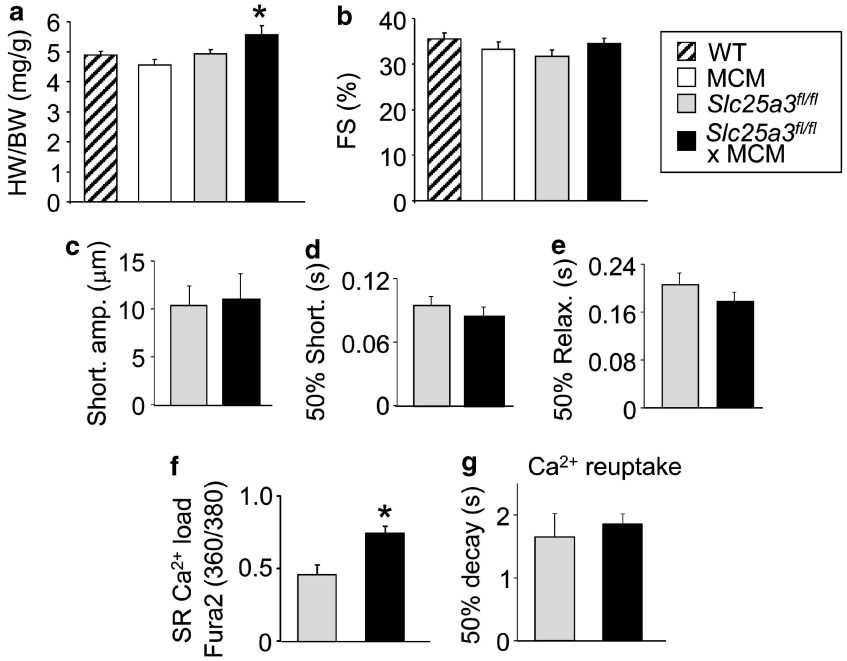

Figure 2 Cardiomyocyte-specific deletion of *Slc25a3* over 2 weeks in young adult mice. (**a**) Heart weight normalized to body weight (HW/BW) of the indicated groups of mice 2 weeks following tamoxifen administration. *$P<0.05$ *versus* all other groups. (**b**) Echocardiographic assessment of fractional shortening (FS%) of mice 2 weeks after tamoxifen treatment. (**c**) Shortening amplitude, (**d**) shortening time (50% time to peak) and (**e**) relaxation time (50% time from peak) in isolated adult cardiomyocytes from the indicated groups 6 weeks following tamoxifen treatment. (**f**) Ca^{2+} transient amplitude after total SR Ca^{2+} release, *$P<0.01$ *versus* all other groups, and (**g**) Ca^{2+} transient decay and reuptake time (50% time from peak) in adult-isolated cardiomyocytes from the indicated groups of mice 10 weeks after tamoxifen treatment. Values reported as mean ± S.E.M. fl/fl, homozygous *Slc25a3-loxP*-targeted mice

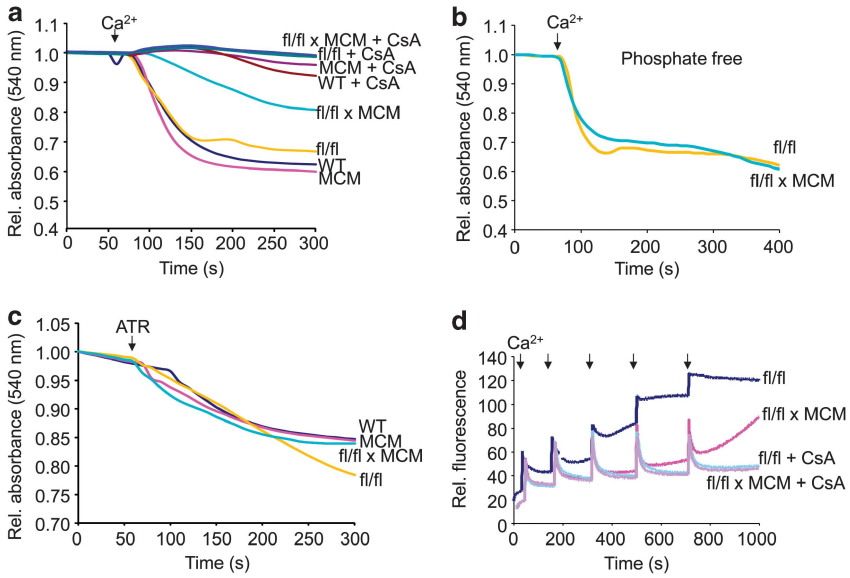

Figure 3 Assessing MPTP function in isolated heart mitochondria from *Slc25a3*-targeted mice. (**a**) Swelling assay in isolated cardiac mitochondria in response to addition of Ca^{2+} in standard phosphate-containing buffer from the genotypes shown. CsA was used as a control for MPTP inhibition. (**b**) Mitochondrial swelling in response to addition of Ca^{2+} in phosphate-free, arsenate-containing buffer for the two genotypes shown. (**c**) Mitochondrial swelling in response to atractyloside (ATR). (**d**) Mitochondrial Ca^{2+} uptake as measured by Ca^{2+} green-5N fluorescence. Representative traces shown from $n=3$. fl/fl, homozygous *Slc25a3-loxP*-targeted mice

suggest that although PiC is not required for MPTP formation, its absence can modulate the sensitivity of the MPTP to Ca^{2+} due to reduced Pi import/levels. We also investigated the ability of mitochondria from hearts of *Slc25a3*$^{fl/fl\text{-}MCM}$ mice to take up Ca^{2+}. The data show that reduction in PiC protein resulted in substantially greater Ca^{2+} uptake capacity, similar to CsA treatment, compared with control mitochondria, further confirming that deletion of *Slc25a3* renders mitochondria less sensitive to Ca^{2+} overload by desensitizing the MPTP (Figure 3d).

To further investigate the ability of PiC to modulate MPTP activity, we also generated mouse embryonic fibroblasts (MEFs) from *Slc25a3*$^{fl/fl}$-targeted mice. These MEFs were treated with either an adenovirus-expressing Cre recombinase (AdCre) to induce *Slc25a3* deletion, or a control adenovirus containing an irrelevant β-galactosidase complementary DNA (Adβgal), the former of which essentially resulted in complete loss of PiC protein (Figure 4a). AdCre-mediated loss of PiC protein partially protected MEFs from a model of ionomycin-induced necrosis through MPTP formation,[22] although CsA was slightly more potent in providing protection (Figure 4b). To directly assess MPTP opening *in vivo*, the calcein–AM–cobalt assay was performed in *Slc25a3*-deleted MEFs (Figure 4c, see methods). Ionomycin-induced Ca^{2+} overload robustly reduced the mitochondrial calcein signal in control MEFs, which indicates MPTP opening (Figure 4c). By contrast, mitochondrial calcein fluorescence was retained for a longer period of time in MEFs lacking PiC protein (Figure 4c). Ablation of PiC in MEFs had no effect on mitochondrial membrane potential ($\Delta\psi$) as measured by Rhod-123 staining (Figure 4d), nor was ROS production altered as measured by MitoSOX Red (Figure 4e). These observations further suggest a role for PiC in modulating the MPTP in living cells.

Consistent with the results in MEFs lacking PiC protein, in which MPTP activity was partially desensitized, thereby conferring protection from programmed necrosis, we also observed partial protection from ischemia-reperfusion (I-R) injury in the hearts of *Slc25a3*$^{fl/fl\text{-}MCM}$ mice. Two weeks following tamoxifen administration, *Slc25a3*$^{fl/fl\text{-}MCM}$, *Slc25a3*$^{fl/fl}$, and α-MHC-MCM mice were subjected to 1 h of cardiac ischemia followed by 24 h of reperfusion. Hearts were then perfused with Evans blue dye, stained with triphenyltetrazolium chloride to show viable myocardium in red, then imaged and analyzed for the amount of cardiac death (Figure 4f). Although the area at risk was similar in all groups (Figure 4g), *Slc25a3*$^{fl/fl\text{-}MCM}$ mice displayed a significant reduction in the area of infarction as compared with controls (Figure 4h). Together, these results suggest that targeted deletion of *Slc25a3* in cells or within the heart desensitizes the MPTP and reduces the extent of programmed necrosis.

Prolonged PiC deletion results in a severe mitochondrial cardiomyopathy. Although cardiac structure and function were relatively normal 2 weeks after *Slc25a3* gene deletion with tamoxifen treatment, by 10 weeks these mice showed severe cardiac hypertrophy and myopathy (Figures 5a and b). Heart weight to body weight ratios were increased by a marked 300% compared with controls (Figure 5c) with a corresponding ~80% increase in myocyte cross-sectional areas (Figure 5d). Echocardiography of hearts from *Slc25a3*$^{fl/fl\text{-}MCM}$ mice 10 weeks after tamoxifen showed significantly reduced fractional shortening with greater left ventricular chamber dimension in diastole (Figures 5e and f). However, Masson's trichrome-stained heart sections showed that loss of PiC did not lead to the development of fibrosis (Supplementary Figure S2a), and correspondingly, there was no change in the percentage of TUNEL-positive

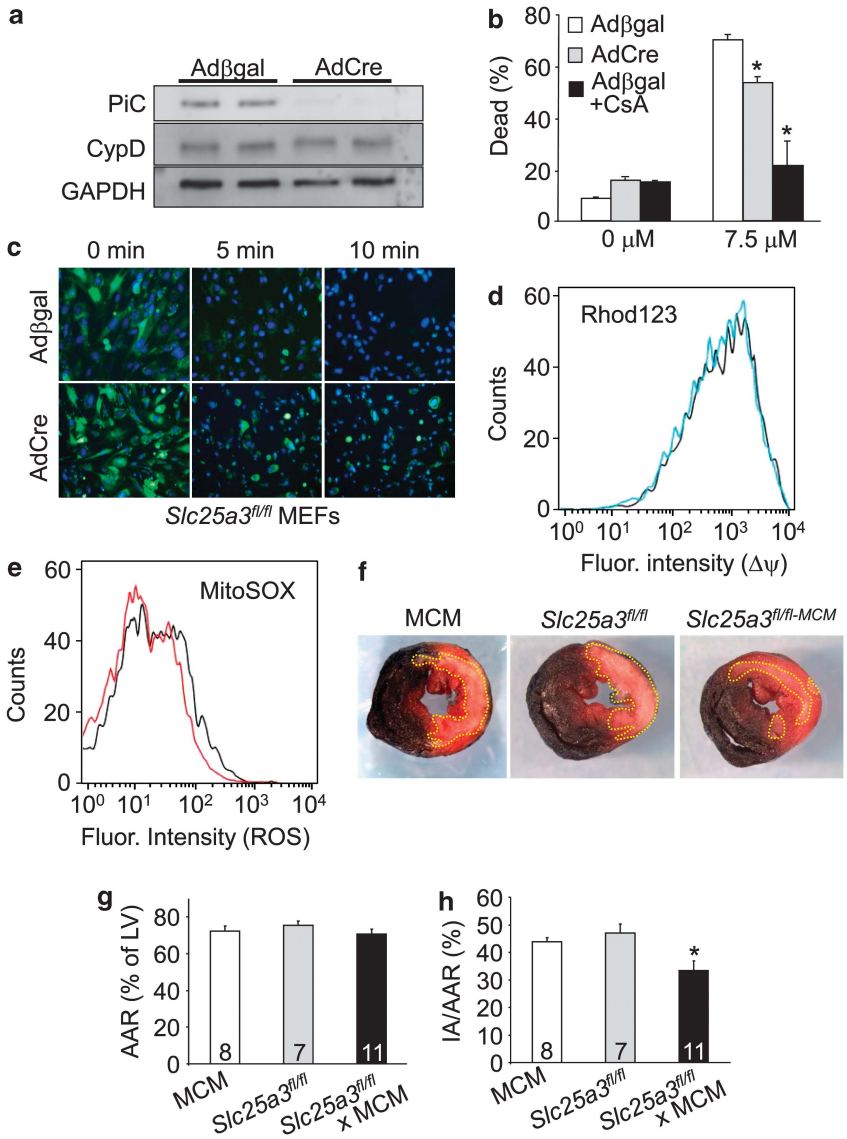

Figure 4 Targeting of *Slc25a3* attenuates cell death. (**a**) Western blot of PiC and CypD protein in cell lysates prepared from *Slc25a3*$^{fl/fl}$ MEFs 72 h after AdCre or Adβgal infection. GAPDH was used as a protein loading control. (**b**) Quantification of cell death (%) in response to ionomycin for 24 h using a live/dead assay kit from Millipore. *$P<0.05$ *versus* Adβgal. (**c**) Representative images of a Calcein-$CoCl_2$ assay in *Slc25a3*$^{fl/fl}$ MEFs treated with the indicated adenoviruses and dosage of ionomycin for the indicated times. (**d**) Rhod-123 measurement of mitochondrial membrane potential ($\Delta\psi$). Representative plots shown from $n=3$. AdCre-transduced MEFs in blue and Adβgal-transduced MEFs in black. (**e**) MitoSOX Red measurement of ROS production in cultured MEFs. Representative plots shown from $n=3$. AdCre-transduced MEFs in red and Adβgal-transduced MEFs in black. (**f**) Representative images of transverse heart sections stained with triphenyltetrazolium chloride (TTC, red area) following ischemia-reperfusion injury. Ischemic area is outlined in yellow. (**g**) Quantification of the percent area at risk (AAR) from hearts described in **f**. (**h**) Quantification of the ischemic area *versus* the area at risk (IA/AAR) for the indicated groups of mice. *$P<0.05$ *versus* all other groups. Number of animals used is shown in the bars. fl/fl, homozygous *Slc25a3-loxP*-targeted mice

cardiomyocytes (Supplementary Figure S2b) with PiC deletion, suggesting that cardiomyocyte death is not a major factor contributing to *Slc25a3* deletion-induced cardiac dysfunction and hypertrophy. Further, examination of hearts from *Slc25a3*$^{fl/fl\text{-}MCM}$ mice by electron microscopy showed extensive sarcomeric disarray with fragmented and disrupted mitochondria, as well as mitochondrial hyperproliferation (Figure 5g). Indeed, direct quantification of mitochondrial DNA content confirmed mitochondrial expansion in the hearts of *Slc25a3*$^{fl/fl\text{-}MCM}$ mice compared with controls (Figure 5h).

The bioenergetic profile of *Slc25a3*$^{fl/fl\text{-}MCM}$ cardiac mitochondria 10 weeks after tamoxifen-induced PiC deletion mirrored that of the 2-week deletion time point, such that protein levels of Pic were down by greater than 95% (Supplementary Figure S3a), and activities of individual respiratory chain complexes were unchanged (Supplementary Figure S3b). However, Ca^{2+}-induced MPTP opening was again blunted in cardiac mitochondria lacking PiC, and mitochondrial Ca^{2+} uptake was similarly enhanced (Supplementary Figures S3c and d). Consistent with these data, *Slc25a3*$^{fl/fl\text{-}MCM}$ cardiac mitochondria continued to show

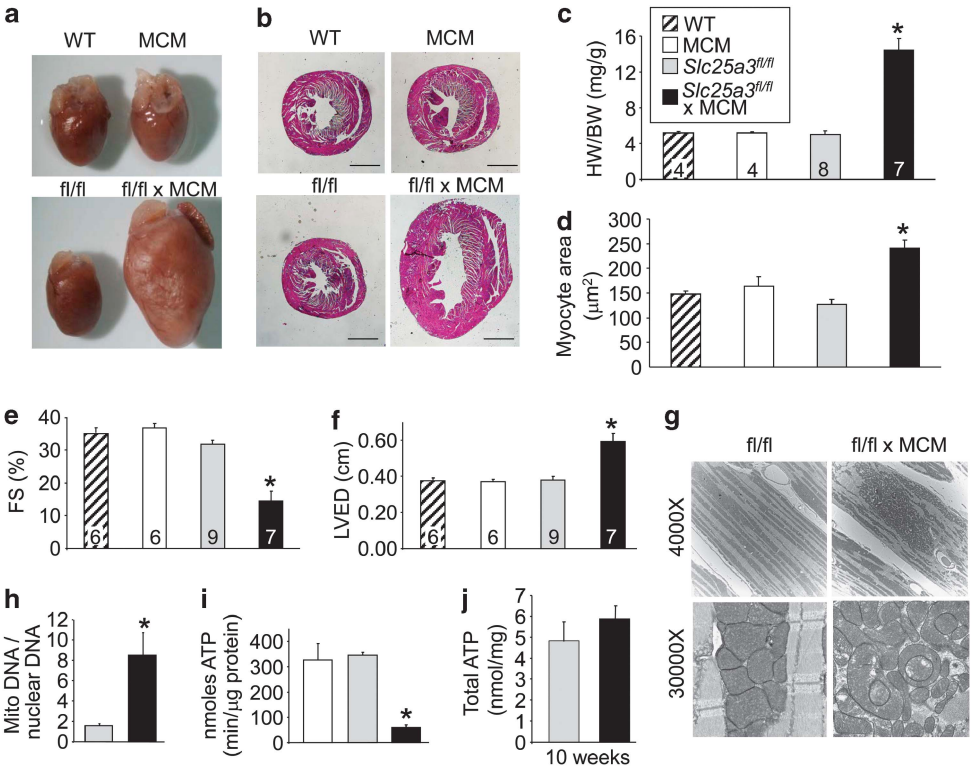

Figure 5 Cardiac-specific deletion of *Slc25a3* over 10 weeks results in severe cardiomyopathy. (**a**) Representative images of whole hearts from the indicated groups of mice 10 weeks after tamoxifen administration. (**b**) Transverse H&E-stained heart sections from the indicated groups. (**c**) Heart weight to body weight (HW/BW) ratios from the indicated groups of mice 10 weeks after tamoxifen administration. *$P<0.005$ *versus* all other groups. (**d**) Quantitative analysis of myocyte cross-sectional area from histological sections of the hearts shown in panel **b**. Greater than 200 myocytes were analyzed per group. *$P<0.05$ *versus* all other groups. (**e** and **f**) Assessment of fractional shortening (FS%) and left ventricular end diastolic dimension (LVED) by echocardiography in the indicated mice, key shown in panel **c**. *$P<0.005$ *versus* all other groups. (**g**) Representative electron micrographs of left ventricular ultrastructure from the genotypes shown. fl/fl denotes *SLC25a3*$^{fl/fl}$ and MCM denotes αMHC-MCM transgene. (**h**) Quantitative PCR of the ratio of mitochondrial to nuclear DNA from whole hearts of the indicated mice. *$P<0.05$ *versus* all control ($n=3$ per group). (**i**) ATP synthesis rates from isolated mitochondria in the indicated groups 10 weeks after tamoxifen treatment ($n=3$ per group). *$P<0.005$ *versus* all other groups. (**j**) Total cardiac tissue ATP content from hearts of the indicated groups 10 weeks after tamoxifen treatment ($n=3$ per group). Values reported as mean ± S.E.M. fl/fl, homozygous *Slc25a3-loxP*-targeted mice

a marked reduction in the rate of ATP synthesis after 10 weeks of gene deletion (Figure 5i). Surprisingly, similar to hearts with the acute 2-week PiC deletion (Figure 1e), the total cardiac tissue ATP levels were unchanged with long-term PiC ablation, suggesting that the myocytes in these hearts were somehow compensating for the reduction in mitochondrial-generated ATP (Figure 5j). To investigate the mechanisms whereby PiC-depleted hearts maintain tissue ATP levels, we analyzed the expression profile of genes involved in glucose metabolism. We found that the cardiac glucose transporters *Slc2a1* and *Slc2a4* were strongly upregulated and expression of a wide range of glycolysis enzymes (*HK1*, *PFKm*, *Gpi1*, *GAPDH*, and *PKM1*) were significantly increased (Supplementary Figure S4). In addition, expression of *PDK4*, an inhibitor of pyruvate entry into the tricarboxylic acid cycle, was greatly increased (Supplementary Figure S4). These results suggest that glucose utilization through glycolysis is enhanced while mitochondrial metabolic flux is reduced as a direct mechanism of compensation for the reduction in mitochondrial ATP production. Collectively, we interpret these results to mean that loss of PiC protein from the heart compromises the ATP synthase's ability to generate adequate ATP, leading to a reactive mitochondrial expansion, upregulation in glycolytic glucose utilization, and induction of hypertrophy as an attempt to maintain cardiac function (see Discussion). Hence, cardiac-specific *Slc25a3*$^{fl/fl\text{-}MCM}$ targeting generates a mouse model of metabolic, mitochondrial cardiomyopathy due to inadequate mitochondrial energy production.

Discussion

Similar to mitochondrial depletion of the MPTP regulator ANT1,[21] we found that cardiac mitochondria lacking PiC protein retained the ability to undergo permeability transition, suggesting that neither protein is a obligate component of the MPTP. However, loss of PiC protein significantly desensitized MPTP opening to Ca^{2+}, as well as led to greater Ca^{2+} uptake capacity at both 2 weeks and 10 weeks after protein deletion. Contrary to previous reports showing that siRNA-mediated partial depletion of PiC in cultured cells had no effect on MPTP opening,[27] we discovered that the complete loss of PiC protein in AdCre-treated *Slc25a3*$^{fl/fl}$ primary MEFs resulted in a delayed dissipation of mitochondrial calcein signal in response to Ca^{2+} challenge, indicative of impaired MPTP function. This state resulted in protection against

ionomycin-induced cell death. Moreover, near complete deletion of cardiac *Slc25a3* produced mitochondria with reduced swelling in response to Ca^{2+}. This impairment in MPTP opening further conferred partial protection against I-R-induced injury to the heart.

In addition to the requirement of Pi for ATP synthesis, Pi is known to serve as an accompanying anion for mitochondrial Ca^{2+} uptake.[29,30] Thus, one possibility for the *Slc25a3* deletion-mediated desensitization of the MPTP is that mitochondrial Ca^{2+} uptake could be impaired. However, we observed that the protective effect of *Slc25a3* deletion was not due to impaired mitochondrial Ca^{2+} uptake, as mitochondria from these gene-targeted mice exhibited an enhanced uptake ability. This finding suggests that PiC's role in regulating the MPTP is not through an effect on Ca^{2+}, but likely due to an effect on the MPTP itself. Indeed, mitochondrial swelling assays conducted in Pi-free buffer no longer showed a reduction in Ca^{2+}-induced swelling from *Slc25a3*-deleted hearts (Figure 3b). This effect may very well be due to Pi, which is an allosteric regulator of the MPTP. Hence loss of PiC protein alters the influx rates of Pi in the microenvironment proximal to the ATPase synthase, which has been suggested to form part of the MPTP. Indeed, PiC, ANT, and the ATP synthase together form the ATP synthasome,[9] thereby more efficiently localizing the supply of substrates for ATP synthesis. Moreover, dimers of the ATP synthase itself, reconstituted *in vitro*, can form a pore with properties similar to the MPTP.[17] ANT1 is also a regulator of the MPTP in much the same way observed for PiC, such that mitochondria from either deficient mouse model take up more Ca^{2+}.[21]

In addition to the finding that PiC modulates MPTP function, we also discovered that long-term deletion of *Slc25a3* in cardiomyocytes results in the development of a severe cardiomyopathy that recapitulates the heart defects observed in humans with *SLC25A3* deficiency.[10,11] Mitochondrial dysfunction can lead to the development of a diverse spectrum of cardiac defects. The cardiomyopathy observed in the *Slc25a3*$^{fl/fl\text{-}MCM}$ mice was specifically characterized by hypertrophy, ventricular dilation, decreased cardiac function, and mitochondrial hyperproliferation with disrupted ultrastructure. Interestingly, this cardiac phenotype is reproduced in mice lacking the gene encoding ANT1 protein.[13,31] Further, the hypertrophic cardiomyopathy observed in *SLC25A3*-deficient patients[10,11] is shared by patients with a recessive loss of function for the *SLC25A4* gene encoding ANT1 protein.[12] Collectively, ANT and PiC may represent two sides of the same coin, as mitochondria lacking either of these proteins share a similar bioenergetic consequence of defective mitochondrial ATP synthesis, resulting in cardiomyopathy in mice and humans. The myocytes sense the reduction in ATP generation capacity from the mitochondria, which leads to a compensatory upregulation in total mitochondrial content and in genes involved in glucose utilization and ATP generation by glycolysis. However, how this lack of mitochondrial ATP generation is sensed by the hypertrophic growth signaling circuitry remains unknown. Our working hypothesis is that under *in vivo* conditions, the lack of PiC causes deficits in ATP concentrations in the heart at the level of the sarcomeres (very difficult to directly measure), leading to alterations in myofilament dynamics and altered tension/relaxation responsiveness. Altered myofilament tension can result in hypertrophic signals and activate disease pathways in the heart.

In conclusion, we have found that the acute genetic ablation of *Slc25a3* desensitizes the MPTP to Ca^{2+} overload and confers protection against cardiac ischemic injury, although PiC is not itself a required component of the MPTP. Thus, PiC represents a possible new avenue to pursue therapeutics to prevent cardiomyocyte death through desensitization of the MPTP. However, as prolonged cardiac *Slc25a3* deletion resulted in mitochondrial cardiomyopathy, our studies highlight the importance that such therapies are applied to short-term injury events, such as after myocardial infarction injury when reperfusion is performed. Finally, as current therapies for mitochondrial diseases are limited, our phosphate carrier-deficient mouse model should provide insight into mitochondrial and energetics-based cardiomyopathies in humans in the hopes of identifying new treatments.

Materials and Methods

Animals. A targeting vector was designed for the *Slc25a3* gene to insert loxP sites flanking exons 1 and 2 for homologous recombination in embryonic stem cells (SV129j background, KG1 cells). Correctly targeted embryonic stem cells were injected into C57Bl/6 blastocysts to generate chimeric mice, which were then bred with C57Bl/6 mice to obtain germline transmission and eventually homozygous targeted mice (*Slc25a3*$^{fl/fl}$). Transgenic mice expressing the tamoxifen-inducible Cre recombinase under the control of α-MHC promoter were described previously.[32] Cre-mediated excision was induced at 2 months of age with tamoxifen (25 mg/kg/day i.p for 5 days). All animal experiments were approved and performed in accordance with Cincinnati Children's Hospital Medical Center's Institutional Animal Care and Use Committee.

Cardiac functional analyses, myocyte isolation, Ca^{2+} handling, and surgeries. Echocardiography was performed using a Hewlett Packard SONOS 5500 instrument (Palo Alto, CA, USA) with a 15-MHz transducer as previously described.[33] I-R injury was performed as previously described.[34] Adult cardiomyocytes were isolated as previously described[35] and myocyte contractility measurements were conducted by video edge detection (Photon Technology International, Birmingham, NJ, USA) as previously described.[36] Functional SR Ca^{2+} load was measured as the Ca^{2+} transient amplitude, resulting from the rapid administration of 20 mM caffeine as previously reported.[37] The decay time of this caffeine-induced contraction was used as an index for the kinetics of cytosolic Ca^{2+} removal. Cardiac ATP content was measured from liquid nitrogen snap frozen hearts using an ATP Determination Kit (Invitrogen, Carlsbad, CA, USA).

Mitochondrial isolation and analyses. Cardiac mitochondria were isolated in MS-EGTA buffer (225 mM mannitol, 75 mM sucrose, 5 mM Hepes, and 1 mM EGTA, pH 7.4) as previously described.[19] Mitochondrial phosphate uptake was measured using a [^{32}P] inhibitor-stop method as described previously.[38] ATP synthesis was measured using an ATP Determination Kit (Invitrogen) with modifications.[39] Mitochondrial swelling was assessed as a measure of light scattering at an absorbance of 540 nm as previously described.[19] Briefly, 250 μg mitochondria were incubated in swelling buffer (120 mM KCl, 10 mM Tris pH 7.4, 5 mM KH_2PO_4, 7 mM pyruvate, 1 mM malate, and 10 μM EDTA) and swelling was initiated with the addition of 200 μM $CaCl_2$ or 200 μM ATR in combination with 25 μM $CaCl_2$. As a control, mitochondria were incubated with 1 μM CsA for 5 min before the start of the assay. For mitochondrial swelling in the presence of arsenate, mitochondria were incubated in buffer containing 120 mM KCl, 10 mM Tris pH 7.4, 5 mM KH_2AsO_4, 7 mM pyruvate, 1 mM malate, and 10 mM EDTA and swelling was initiated with the addition of 400 μM $CaCl_2$. Mitochondrial Ca^{2+} uptake was measured using Calcium Green 5N (Molecular Probes, Eugene, OR, USA) in a Synergy 2 Multi-Mode Microplate Reader (BioTek, Winooski, VT, USA).[40] For this assay, mitochondria were sequentially challenged with additions of $CaCl_2$ (12.5 mM) and fluorescence was monitored. The activities of the individual respiratory chain complexes I–IV were measured in isolated cardiac

mitochondria as previously described.[41] Complex V activity was measured spectrophotometrically as a function of ATP hydrolysis coupled to NADH oxidation using the Mitochondrial Complex V Activity Assay kit (EMD Millipore, Billerica, MA, USA). Mitochondrial free radical production was measured under energized conditions (7 mM pyruvate and 1 mM malate) using the Amplex Red Hydrogen Peroxide/Peroxidase Assay Kit (Invitrogen) as described in.[42] To quantify mitochondrial DNA content, quantitative PCR was performed for the *mt-Nd5* gene (mitochondrial) *versus* the 18S rRNA subunit (nuclear).

Cell culture and adenoviral infection. MEFs were isolated from *Slc25a3*$^{fl/fl}$ E13.5 embryos and grown under conditions for culturing cells with mitochondrial dysfunction (Dulbeco's modified Eagle media containing 10% fetal bovine serum, 4.5 g/l glucose, 1 mM pyruvate, and 50 μg/ml uridine).[40,43] MEFs were transduced with adenoviruses for 72 h. Cell death was induced with ionomycin as previously described.[22] Cell viability was measured using the Muse Cell Analyzer (EMD Millipore). Mitochondrial membrane potential was measured with Rhodamine-123 (Rhod-123, Life Technologies, Carlsbad, CA, USA). MEFs were incubated with 25 μM Rhod-123 and fluorescence was quantified by FACS analysis (BD FACSCalibur, BD Biosciences, Franklin Lakes, NJ, USA). Mitochondrial superoxide production was measured with the MitoSOX kit (Life Technologies). MEFs were stained with 5 μM MitoSOX and fluorescence was quantified by FACS analysis.

RT-PCR and TUNEL. Cardiac RNA was purified using the RNeasy Fibrous Tissue Mini Kit (Qiagen, Venlo, Netherlands) and cDNA was prepared using the First Strand Synthesis Kit (Invitrogen). Primer sequences for target genes were obtained from PrimerBank.[44] TUNEL staining was performed using the *In Situ* Cell Detection Kit (Roche, Basel, Switzerland).

Statistical analyses. All results are presented as mean S.E.M. *P*-values <0.05 were considered significant as assessed by student's *t*-test.

Conflict of Interest

The authors declare no conflict of interest.

Acknowledgements. This work was supported by grants from the National Institutes of Health and the Howard Hughes Medical Institute (to JDM). JQK was supported by an American Heart Association postdoctoral fellowship from the Great Rivers Affiliate.

1. Skladal D, Halliday J, Thorburn DR. Minimum birth prevalence of mitochondrial respiratory chain disorders in children. *Brain* 2003; **126**: 1905–1912.
2. Vafai SB, Mootha VK. Mitochondrial disorders as windows into an ancient organelle. *Nature* 2012; **491**: 374–383.
3. Zaragoza MV, Brandon MC, Diegoli M, Arbustini E, Wallace DC. Mitochondrial cardiomyopathies: how to identify candidate pathogenic mutations by mitochondrial DNA sequencing, MITOMASTER and phylogeny. *Eur J Hum Genet* 2011; **19**: 200–207.
4. Brega A, Narula J, Arbustini E. Functional, structural, and genetic mitochondrial abnormalities in myocardial diseases. *J Nucl Cardiol* 2001; **8**: 89–97.
5. DiMauro S, Hirano M. Mitochondria and heart disease. *Curr Opin Cardiol* 1998; **13**: 190–197.
6. Kolbe HV, Costello D, Wong A, Lu RC, Wohlrab H. Mitochondrial phosphate transport. Large scale isolation and characterization of the phosphate transport protein from beef heart mitochondria. *J Biol Chem* 1984; **259**: 9115–9120.
7. Palmieri F. The mitochondrial transporter family (SLC25): physiological and pathological implications. *Pflugers Arch* 2004; **447**: 689–709.
8. Ko YH, Delannoy M, Hullihen J, Chiu W, Pedersen PL. Mitochondrial ATP synthasome. Cristae-enriched membranes and a multiwell detergent screening assay yield dispersed single complexes containing the ATP synthase and carriers for Pi and ADP/ATP. *J Biol Chem* 2003; **278**: 12305–12309.
9. Chen C, Ko Y, Delannoy M, Ludtke SJ, Chiu W, Pedersen PL. Mitochondrial ATP synthasome: three-dimensional structure by electron microscopy of the ATP synthase in complex formation with carriers for Pi and ADP/ATP. *J Biol Chem* 2004; **279**: 31761–31768.
10. Mayr JA, Zimmermann FA, Horvath R, Schneider HC, Schoser B, Holinski-Feder E *et al.* Deficiency of the mitochondrial phosphate carrier presenting as myopathy and cardiomyopathy in a family with three affected children. *Neuromuscul Disord* 2011; **21**: 803–808.
11. Mayr JA, Merkel O, Kohlwein SD, Gebhardt BR, Bohles H, Fotschl U *et al.* Mitochondrial phosphate-carrier deficiency: a novel disorder of oxidative phosphorylation. *Am J Hum Genet* 2007; **80**: 478–484.
12. Palmieri L, Alberio S, Pisano I, Lodi T, Meznaric-Petrusa M, Zidar J *et al.* Complete loss-of-function of the heart/muscle-specific adenine nucleotide translocator is associated with mitochondrial myopathy and cardiomyopathy. *Hum Mol Genet* 2005; **14**: 3079–3088.
13. Graham BH, Waymire KG, Cottrell B, Trounce IA, MacGregor GR, Wallace DC. A mouse model for mitochondrial myopathy and cardiomyopathy resulting from a deficiency in the heart/muscle isoform of the adenine nucleotide translocator. *Nat Genet* 1997; **16**: 226–234.
14. Alcala S, Klee M, Fernandez J, Fleischer A, Pimentel-Muinos FX. A high-throughput screening for mammalian cell death effectors identifies the mitochondrial phosphate carrier as a regulator of cytochrome c release. *Oncogene* 2008; **27**: 44–54.
15. Halestrap AP. What is the mitochondrial permeability transition pore? *J Mol Cell Cardiol* 2009; **46**: 821–831.
16. Leung AW, Varanyuwatana P, Halestrap AP. The mitochondrial phosphate carrier interacts with cyclophilin D and may play a key role in the permeability transition. *J Biol Chem* 2008; **283**: 26312–26323.
17. Giorgio V, von Stockum S, Antoniel M, Fabbro A, Fogolari F, Forte M *et al.* Dimers of mitochondrial ATP synthase form the permeability transition pore. *Proc Natl Acad Sci USA* 2013; **110**: 5887–5892.
18. Bonora M, Bononi A, De Marchi E, Giorgi C, Lebiedzinska M, Marchi S *et al.* Role of the c subunit of the FO ATP synthase in mitochondrial permeability transition. *Cell Cycle* 2013; **12**: 674–683.
19. Baines CP, Kaiser RA, Purcell NH, Blair NS, Osinska H, Hambleton MA *et al.* Loss of cyclophilin D reveals a critical role for mitochondrial permeability transition in cell death. *Nature* 2005; **434**: 658–662.
20. Nakagawa T, Shimizu S, Watanabe T, Yamaguchi O, Otsu K, Yamagata H *et al.* Cyclophilin D-dependent mitochondrial permeability transition regulates some necrotic but not apoptotic cell death. *Nature* 2005; **434**: 652–658.
21. Kokoszka JE, Waymire KG, Levy SE, Sligh JE, Cai J, Jones DP *et al.* The ADP/ATP translocator is not essential for the mitochondrial permeability transition pore. *Nature* 2004; **427**: 461–465.
22. Karch J, Kwong JQ, Burr AR, Sargent MA, Elrod JW, Peixoto PM *et al.* Bax and Bak function as the outer membrane component of the mitochondrial permeability pore in regulating necrotic cell death in mice. *Elife* 2013; **2**: e00772.
23. Whelan RS, Konstantinidis K, Wei AC, Chen Y, Reyna DE, Jha S *et al.* Bax regulates primary necrosis through mitochondrial dynamics. *Proc Natl Acad Sci USA* 2012; **109**: 6566–6571.
24. Beatrice MC, Palmer JW, Pfeiffer DR. The relationship between mitochondrial membrane permeability, membrane potential, and the retention of Ca2 + by mitochondria. *J Biol Chem* 1980; **255**: 8663–8671.
25. Al-Nasser I, Crompton M. The reversible Ca2 +-induced permeabilization of rat liver mitochondria. *Biochem J* 1986; **239**: 19–29.
26. Crompton M, Costi A. Kinetic evidence for a heart mitochondrial pore activated by Ca2 +, inorganic phosphate and oxidative stress. A potential mechanism for mitochondrial dysfunction during cellular Ca2 + overload. *Eur J Biochem* 1988; **178**: 489–501.
27. Varanyuwatana P, Halestrap AP. The roles of phosphate and the phosphate carrier in the mitochondrial permeability transition pore. *Mitochondrion* 2012; **12**: 120–125.
28. Gutierrez-Aguilar M, Perez-Martinez X, Chavez E, Uribe-Carvajal S. In *Saccharomyces cerevisiae*, the phosphate carrier is a component of the mitochondrial unselective channel. *Arch Biochem Biophys* 2010; **494**: 184–191.
29. Lehninger AL. Role of phosphate and other proton-donating anions in respiration-coupled transport of Ca2 + by mitochondria. *Proc Natl Acad Sci USA* 1974; **71**: 1520–1524.
30. Lehninger AL, Carafoli E, Rossi CS. Energy-linked ion movements in mitochondrial systems. *Adv Enzymol Relat Areas Mol Biol* 1967; **29**: 259–320.
31. Narula N, Zaragoza MV, Sengupta PP, Li P, Haider N, Verjans J *et al.* Adenine nucleotide translocase 1 deficiency results in dilated cardiomyopathy with defects in myocardial mechanics, histopathological alterations, and activation of apoptosis. *JACC Cardiovasc Imaging* 2011; **4**: 1–10.
32. Sohal DS, Nghiem M, Crackower MA, Witt SA, Kimball TR, Tymitz KM *et al.* Temporally regulated and tissue-specific gene manipulations in the adult and embryonic heart using a tamoxifen-inducible Cre protein. *Circ Res* 2001; **89**: 20–25.
33. Nakayama H, Bodi I, Correll RN, Chen X, Lorenz J, Houser SR *et al.* alpha1G-dependent T-type Ca2 + current antagonizes cardiac hypertrophy through a NOS3-dependent mechanism in mice. *J Clin Invest* 2009; **119**: 3787–3796.
34. Kaiser RA, Bueno OF, Lips DJ, Doevendans PA, Jones F, Kimball TF *et al.* Targeted inhibition of p38 mitogen-activated protein kinase antagonizes cardiac injury and cell death following ischemia-reperfusion in vivo. *J Biol Chem* 2004; **279**: 15524–15530.
35. Goonasekera SA, Hammer K, Auger-Messier M, Bodi I, Chen X, Zhang H *et al.* Decreased cardiac L-type Ca(2)(+) channel activity induces hypertrophy and heart failure in mice. *J Clin Invest* 2012; **122**: 280–290.
36. Maillet M, Davis J, Auger-Messier M, York A, Osinska H, Piquereau J *et al.* Heart-specific deletion of CnB1 reveals multiple mechanisms whereby calcineurin regulates cardiac growth and function. *J Biol Chem* 2010; **285**: 6716–6724.

37. Bassani RA, Bassani JW, Bers DM. Mitochondrial and sarcolemmal Ca2 + transport reduce [Ca2 +]i during caffeine contractures in rabbit cardiac myocytes. *J Physiol* 1992; **453**: 591–608.
38. Paradies G, Ruggiero FM. Effect of aging on the activity of the phosphate carrier and on the lipid composition in rat liver mitochondria. *Arch Biochem Biophys* 1991; **284**: 332–337.
39. Vives-Bauza C, Yang L, Manfredi G. Assay of mitochondrial ATP synthesis in animal cells and tissues. *Methods Cell Biol* 2007; **80**: 155–171.
40. Kwong JQ, Henning MS, Starkov AA, Manfredi G. The mitochondrial respiratory chain is a modulator of apoptosis. *J Cell Biol* 2007; **179**: 1163–1177.
41. Tang S, Le PK, Tse S, Wallace DC, Huang T. Heterozygous mutation of Opa1 in Drosophila shortens lifespan mediated through increased reactive oxygen species production. *PLoS One* 2009; **4**: e4492.
42. Starkov AA. Measurement of mitochondrial ROS production. *Methods Mol Biol* 2010; **648**: 245–255.
43. King MP, Attardi G. Human cells lacking mtDNA: repopulation with exogenous mitochondria by complementation. *Science* 1989; **246**: 500–503.
44. Spandidos A, Wang X, Wang H, Seed B. PrimerBank: a resource of human and mouse PCR primer pairs for gene expression detection and quantification. *Nucleic Acids Res* 2010; **38**: D792–D799.

Supplementary Information accompanies this paper on Cell Death and Differentiation website (http://www.nature.com/cdd)